EAST EUROPEAN JOURNAL OF PHYSICS. 3. 436-441 (2025)
DOI:10.26565/2312-4334-2025-3-47 ISSN 2312-4334

ANALYSIS OF TEMPERATURE-DEPENDENT SURFACE PROPERTIES IN THE Ni/SiO_2/Si SYSTEM DURING ELECTRON BEAM DEPOSITION

A.A. Rakhimov, I.Kh. Khudaykulov*, A.A. Ismatov, M.M. Adilov
U.A. Arifov Institute of Ion-Plasma and Laser Technologies, Academy of Sciences of Uzbekistan
100125, Durmon Yuli str. 33, Tashkent, Uzbekistan
**Corresponding Author E-mail: i_khudaykulov@mail.ru*
Received May 8, 2025; revised June 7, 2025; accepted July 29, 2025

In this study, we investigated the morphological properties of nickel (Ni) island-shaped thin films formed on a SiO_x/Si substrate using the electron beam evaporation method. The morphology was examined using Scanning Electron Microscopy (SEM) and Atomic Force Microscopy (AFM). SEM images were analyzed using ImageJ software to determine the size, density, distribution, and coverage ratio of the islands. The results showed a strong dependence of island morphology on substrate temperature: at 20 °C, the islands had an irregular shape with a density of 103 μm^{-2}, while at 250°C and 500°C, the islands became more spherical in shape, and their densities increased to 751.8 and 1212.4 μm^{-2}, respectively. AFM analysis confirmed the uniform distribution of the islands and their average height (15.4 nm). EDS analysis revealed the presence and uniform distribution of Si, O, and Ni elements on the surface. These findings confirm that substrate temperature is a critical factor in the island formation process.
Keywords: *Nickel nanoparticles; Silicon oxide; Electron beam physical vapor deposition; Layer morphology; Vacuum; Substrate surface; Nanocatalyst*
PACS: 81.15.-z; 68.47.Fg

1. INTRODUCTION

Nickel nanoparticles and thin films possess unique physical and chemical properties that ensure high efficiency and have a wide range of applications. Specifically, they are effectively used in the synthesis of carbon nanotubes [1], hydrogenation [2] and oxidation reactions [3], spintronics [4], electronics [5], magnetic devices [6], as well as energy storage systems [7] and sensor devices [8].

These applications are mainly attributed to the high catalytic activity, thermal and chemical stability, and distinctive electronic structure of nickel nanoparticles [9]. Nickel nanoparticles embedded in an oxide matrix provide a valuable platform for in-depth investigation of various physical phenomena. Compared to bulk nickel metal, oxide-supported nickel nanoparticles exhibit different catalytic activity, stability, and electronic properties [10]. These features are especially important in heterogeneous catalysis processes [11]. Among the key factors influencing catalytic performance, the composition of the support material, as well as the size and shape of the nanoclusters, deserve special attention [12].

Research shows that these factors can significantly alter the reactivity and thermodynamic stability of nickel nanoparticles [12]. Therefore, controlling the size and shape of nickel catalyst particles during their growth process is one of the key challenges [13]. Currently, buffer layers formed on SiO_x substrates play a crucial role in regulating the growth mechanism of metal nanoparticles. These layers help manage the chemical and physical interactions between the substrate and metal nanoparticles [14]. At the same time, they contribute to improving the morphological and crystalline structure of the nanoparticles [15]. Buffer layers based on oxide play an important role in the formation of nanostructured materials. In particular, nickel nanoparticles grown on a SiO_x surface exhibit high dispersion, which facilitates an increase in their activity [16].

Moreover, these layers play an important role in determining the chemical composition, electronic properties, and thermodynamic stability of the nanoparticles [17]. The primary objective of this study is to investigate the growth mechanisms of nickel nanoparticles from the vapor phase via electron beam evaporation on a SiO_x buffer layer surface. This involves examining the formation process of Ni nanoparticles, as well as their morphological and structural characteristics depending on the substrate temperature. Additionally, the study explores how the synthesis conditions influence the formation and controllability of the nanoparticles' properties [18]. The obtained results are expected to contribute to a deeper understanding of nickel nanoparticle formation within oxide-based buffer layer matrices. Furthermore, the study aims to identify more efficient ways to control nanoparticle formation processes based on these mechanisms. The findings will serve as a valuable scientific foundation for applications in catalytic processes and nanomaterials engineering.

2. EXPERIMENTAL

A monocrystalline Si (111) wafer was used as the substrate. To remove various organic compounds from the surface, the substrate was first immersed in acetone ($(CH_3)_2CO$) and methanol (CH_3OH) baths at a temperature of 55°C for 15 minutes. It was then rinsed with deionized water and dried under a nitrogen atmosphere. To form an oxide layer on the

Cite as: A.A. Rakhimov, I.Kh. Khudaykulov, A.A. Ismatov, M.M. Adilov, East Eur. J. Phys. 3, 436 (2025), https://doi.org/10.26565/2312-4334-2025-3-47

silicon substrate, it was annealed in a SNOL furnace at 1000 °C for two hours. The thickness of the resulting SiOx layer was analyzed using a SER-850 model spectral ellipsometer manufactured by SENTECH. Based on the Cauchy layer model, the measurements showed that the thickness of the SiOx layer was 60 nm.

In the present study, a thin nickel island layer was deposited onto the SiO_x/Si substrate via electron beam physical vapor deposition (EB-PVD). This method enables high-purity film growth under controlled vacuum conditions. The schematic diagram of the deposition setup used in the experiment is presented in Figure 1.

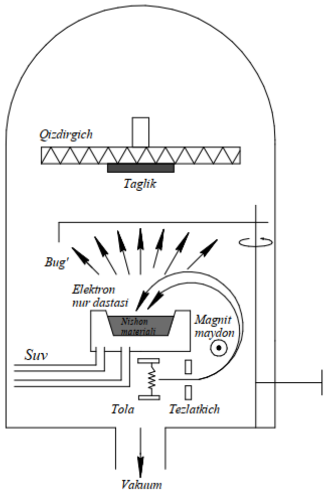

Figure 1. Schematic representation of the thin film deposition process via electron beams physical vapor deposition (EB-PVD)

The device is equipped with an electron beam evaporation system (model SEB-06) with a power capacity of 6 kW, capable of operating with an external voltage of up to 10 kV and an electron emission current of up to 600 mA. A high vacuum of up to 10^{-8} Torr is achieved in the chamber using a turbomolecular pump. This minimizes the contribution of impurities from the sample and the crucible during the evaporation process. Nickel (Ni) vapor was deposited onto the substrate surface under a vacuum of 10^{-6} Torr, using an electron beam with a current of 30 mA and a voltage of 10 kV for a duration of 3 seconds.

The surface morphology of the obtained thin films was studied using a Thermo Fisher Scientific (Apreo 2S SEM). During the investigation, accelerating voltages ranging from 2 kV to 20 kV were used. Low accelerating voltage (2 kV) was applied to obtain surface morphological images of the sample, while high voltage (20 kV) was used for elemental composition analysis. SEM images were captured at various magnification levels (from ×5,000 to ×100,000), allowing the assessment of film uniformity and the identification of potential structural anomalies on the surface.

3. RESULTS AND DISCUSSION

To evaluate the surface morphology of the samples, scanning electron microscopy (SEM) analyses were performed. The ImageJ software was used to determine the size and surface distribution of Ni islands from the SEM images. This software allows for the identification of individual island areas and quantities within the image, which in turn helps calculate the island diameter, surface density, and coverage coefficient. Figure 1 shows the SEM images of the Ni island structure grown on SiO/Si at different substrate temperatures (20°C, 250°C, and 500°C) for 4 seconds. The shape of the islands was idealized as spherical, and their diameters were determined. The histograms of Ni nanoparticles diameters were displayed in Figure 1(d-f).

Figure 1(a) shows the SEM image of the surface morphology of the Ni island structure formed at a substrate temperature of 20°C using the electron beam heating method. It can be seen that the islands have an irregular shape and are arranged in a way that they are not entirely separated from each other.

The values of parameters such as the diameter, area, surface density, and surface coverage ratio of Ni nanoparticles obtained from the SEM images (a–c) in Figure 1 using the ImageJ software are presented in Table 1. Using the ImageJ software for image analysis, the average diameter of the islands was found to be 52.9 nm, and the surface density was 103 μm^{-2}. These values indicate that at low temperatures, the mobility of metal atoms is limited. As a result, many voids may form in the structure. For this reason, the islands are unevenly distributed on the substrate and have an irregular shape.

Table 1. Results of SEM analysis for the size and surface density of Ni island structures grown on the substrate at 20°C, 250°C, and 500°C temperatures.

SiO_x/Si temperature (^{0}C)	**Area (10^{-4} μm^2)**	**Diameter (nm)**	**Density (μm^{-2})**	**Coverage (%)**
20	21.9±7.2	52.9	103±0.2	62.70
250	5.81±2.8	27.2	751.8±0.4	43.610
500	**2.3±1.2**	**17.3**	**1212.4±0.3**	**28.7**

In Figure 1(b), it is observed that as the substrate temperature increased up to 250°C during the deposition process, the shape of the islands became more orderly, approaching a spherical form. At this temperature, the mobility of atoms increases, causing them to start approaching a more energetically stable configuration, that is, transitioning to a shape that minimizes surface energy. According to the analysis results, at 250°C, the average diameter of the islands decreased to 27.2 nm, and the surface density increased to 751 μm^{-2}, with the islands being fully separated from each other and evenly distributed across the surface.

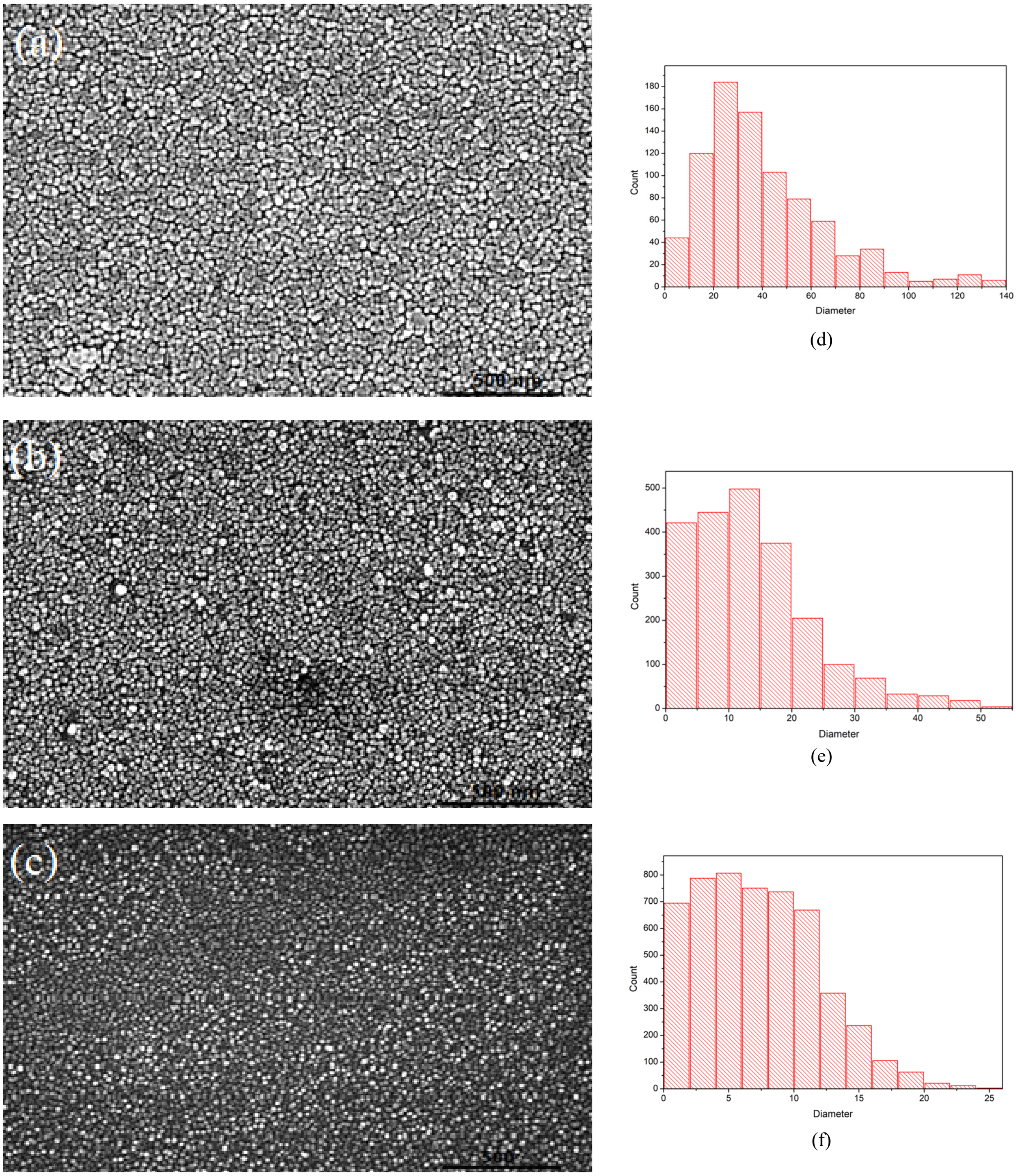

Figure 1. SEM images of Ni nanoparticles formed on the SiO_x/Si substrate surface at substrate temperatures of 20°C, 250°C, and 500°C and and the histograms of Ni nanoparticles diameters (a, b, s). Scale bar – 500 nm.

In Figure 1(c), at a substrate temperature of 500°C during the deposition process, the size of the islands further decreased, with the average diameter reaching 17.3 nm and the surface density increasing to 1212 μm^{-2}. These results indicate that at higher temperatures, the activation of atomic diffusion leads to an increase in the number of islands and a decrease in their size.

Furthermore, the coverage ratio of the islands was found to vary with the substrate temperature. Specifically, the coverage coefficient was 42.7% at 20°C, 46.3% at 250°C, and 48.9% at 500°C. This indicates that as the temperature increases, both the density of the islands and the overall surface coverage increase. These analyses confirm that substrate temperature is a decisive factor in the process of metal island formation.

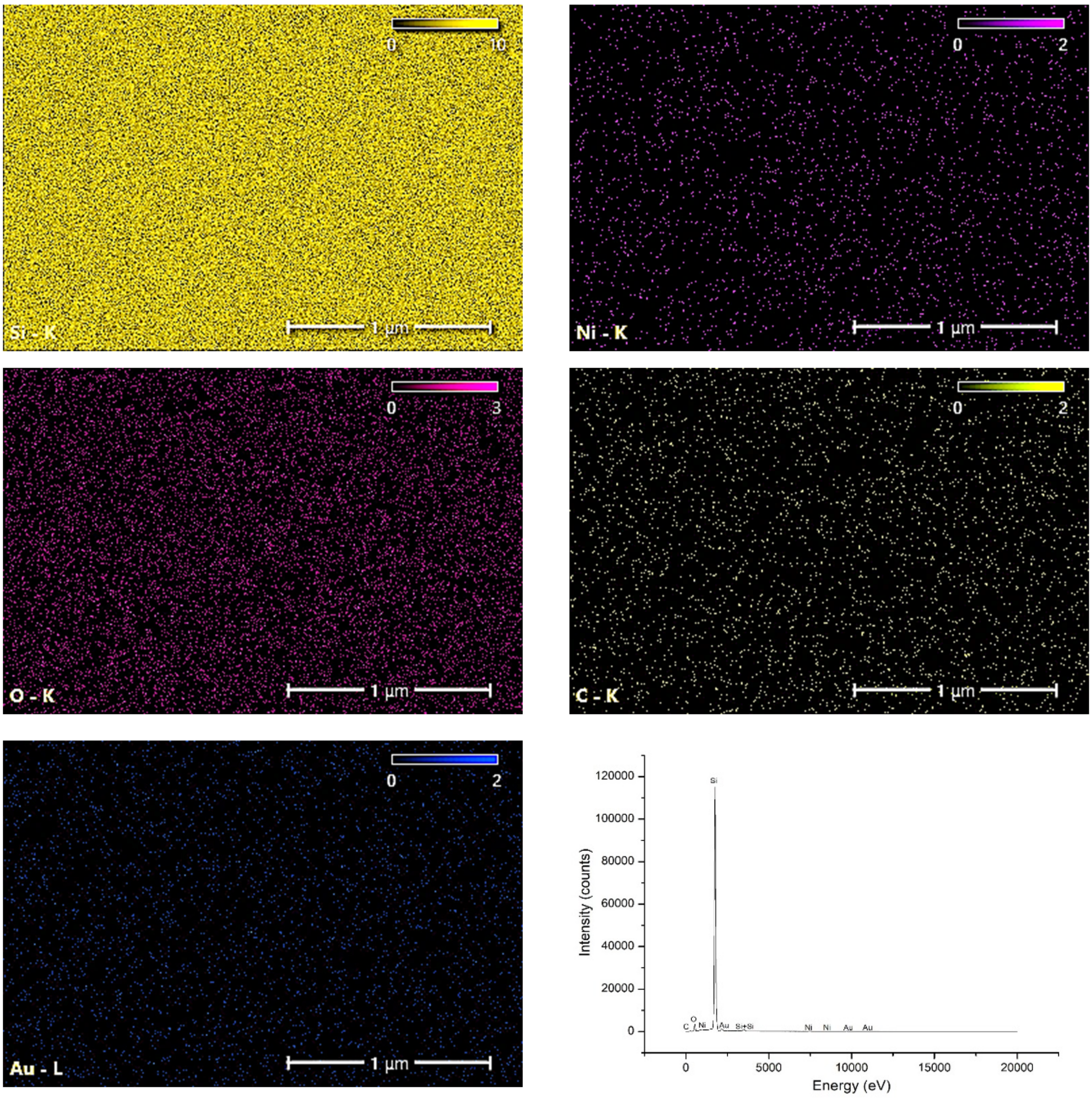

Figure 2. Elemental mapping/EDS spectrum of $Ni/SiO_x/Si$

Energy dispersive spectroscopy (EDS) analysis was performed on a sample grown at a substrate temperature of 250°C to determine the chemical composition of the $Ni/SiO_x/Si$ structure. This analysis allowed for the determination of the elemental composition in the sample as well as their distribution across the surface.

According to the EDS elemental mapping results, the presence of silicon (Si), oxygen (O), and nickel (Ni) elements in the Ni/SiO/Si structure was confirmed, and their uniform distribution across the substrate surface was observed. Specifically, it was noted that nickel nanoparticles and their aggregates were not localized but were almost uniformly distributed on the sample surface.

The Au element identified in the EDS spectrum was deposited on the sample surface in a very thin (3 nm) layer prior to analysis. Its purpose is to enhance the SEM image quality and contrast, as well as to improve the electrical conductivity of the sample. This is a standard practice widely used in SEM analyses. The presence of carbon (C) observed in the spectrum is mainly explained by the effect of the carbon tape used to attach the sample during the SEM analysis. That is, the C element is not a constituent part of the sample itself, but is present in the composition due to the technical support material. Based on the EDS spectrum, the atomic percentages of the identified elements were determined as follows: Si - 70.7%, O - 16.3%, C - 11.2%, Ni - 1.3%, and Au - 0.4%.

It was determined that the main composition of the sample consists of Si and O elements, indicating the dominance of the SiO_x substrate. The relatively small amount of Ni nanoparticles is located in the upper parts of the layer, and it is these that play a key role in morphological analysis and determining functional properties. In general, the results of the EDS analysis, in agreement with the SEM and AFM analyses presented above, qualitatively explained the presence or absence of foreign impurities, reflecting the elemental composition in the Ni/SiO_x/Si structure.

To further assess the surface unevenness of the Ni island structure and the spatial distribution of the islands, Atomic Force Microscopy (AFM) analysis was conducted. The 3D AFM image (Figure 3) provided detailed information about the surface topography and roughness of the Ni/SiO/Si sample, which was obtained at a substrate temperature of 250°C.

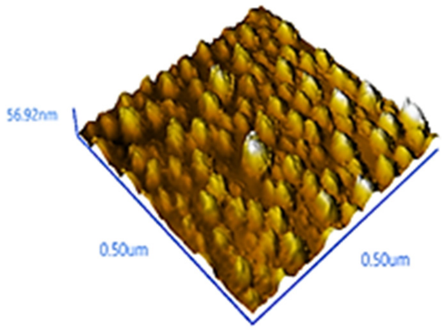

Figure 3. 3D topographic AFM image for the Ni/SiO/Si sample

The image reveals that the distribution of the Ni islands across the substrate surface is relatively uniform and exhibits a clear structure. The islands are located close to each other, with some of them not fully separated, forming a dense mass. This observation aligns with the results from the SEM analysis, showing that the islands exhibit irregular shapes and vary somewhat in size. The height profile from the AFM image indicates that the surface roughness is relatively stable, with minimal variations between individual islands. The average height (Rm) of the Ni islands was found to be approximately 15.4 nm. This suggests that the surface relief of the thin film does not have significant differences between peaks and valleys, and the islands grew at nearly the same height. These findings are consistent with the data obtained from the SEM analysis, demonstrating that at higher substrate temperatures, Ni islands adopt a more uniform shape and higher density distribution.

4. CONCLUSIONS

In this study, the morphological characteristics of Ni island-shaped thin films formed on the SiO/Si substrate surface using the electron beam physical vapor deposition (EB-PVD) method were investigated through scanning electron microscopy (SEM) and atomic force microscopy (AFM) techniques. Data obtained from SEM images using the ImageJ software allowed for the determination of the islands' size, surface distribution, density, and coverage coefficient. According to the results, the geometric parameters and distribution of the Ni islands were directly dependent on the substrate temperature. At a temperature of 20 °C, the islands exhibited irregular shapes and were located close to each other, with an average diameter of 52.9 nm and a density of 103 μm^{-2}. As the temperature increased to 250°C and 500°C, the shape of the islands became closer to spherical, their size decreased, and their density increased to 751.8 μm^{-2} and 1212.4 μm^{-2}, respectively. These changes were attributed to the islands striving for a thermodynamically stable state and minimizing the surface energy. Moreover, AFM images confirmed that the islands were evenly distributed on the surface, with an average height of approximately 15.4 nm. The elemental composition was determined using EDS analysis, which showed the presence of Si, O, and Ni elements on the surface, evenly distributed. Thus, the results of the study demonstrated that the morphology and surface properties of the Ni island structure are strongly dependent on the substrate temperature.

Funding

The authors gratefully acknowledge the financial and technical support provided by the Ministry of Higher Education, Science, and Innovation under project number IL-5421101842.

ORCID

I.Kh. Khudaykulov, https://orcid.org/0000-0002-2335-4456; **M.M. Adilov,** https://orcid.org/0000-0003-0312-2356

REFERENCES

[1] J. Cheng, X. Zhang, and Y. Ye, "Synthesis of nickel nanoparticles and carbon encapsulated nickel nanoparticles supported on carbon nanotubes," Journal of Solid-State Chemistry, **179**(1), 91-95 (2006). https://doi.org/10.1016/j.jssc.2005.10.001

[2] J. Xia, G. He, L. Zhang, X. Sun, and X. Wang, "Hydrogenation of nitrophenols catalyzed by carbon black-supported nickel nanoparticles under mild conditions," Applied Catalysis B: Environmental, **180**, 408-415 (2016). https://doi.org/10.1016/j.apcatb.2015.06.043

[3] A. Singh, S.L. Chang, R.K. Hocking, U. Bach, and L. Spiccia, "Highly active nickel oxide water oxidation catalysts deposited from molecular complexes," Energy & Environmental Science, **6**(2), 579-586 (2013). https://doi.org/10.1039/C2EE23862D

[4] J. Mroziński, "New trends of molecular magnetism," Coordination chemistry reviews, **249**(21-22), 2534-2548 (2005). https://doi.org/10.1016/j.ccr.2005.05.013

[5] R. Poulain, G. Lumbeeck, J. Hunka, J. Proost, H. Savolainen, H. Idrissi, *et al*., "Electronic and chemical properties of nickel oxide thin films and the intrinsic defects compensation mechanism," ACS Applied Electronic Materials, **4**(6), 2718-2728 (2022). https://doi.org/10.1021/acsaelm.2c00230
[6] S. Nadaf, G.K. Jena, N. Rarokar, N. Gurav, M. Ayyanar, S. Prasad, and S. Gurav, "Biogenic and biomimetic functionalized magnetic nanosystem: Synthesis, properties, and biomedical applications," Hybrid Advances, **3**, 100038 (2023). https://doi.org/10.1016/j.hybadv.2023.100038
[7] D. Zhou, X. Guo, Q. Zhang, Y. Shi, H. Zhang, C. Yu, and H. Pang, "Nickel-based materials for advanced rechargeable batteries," Advanced Functional Materials, **32**(12), 2107928 (2022). https://doi.org/10.1002/adfm.202107928
[8] S.G. Danjumma, Y. Abubakar, and S. Suleiman, "Nickel oxide (NiO) devices and applications: a review," J. Eng. Res. Technol, **8**, 12-21 (2019). https://doi.org/10.17577/IJERTV8IS040281
[9] B. Han, B. Yu, J. Wang, M. Liu, G. Gao, K. Xia, *et al*., "Understanding the electronic metal-support interactions of the supported Ni cluster for the catalytic hydrogenation of ethylene," Molecular Catalysis, **511**, 111731 (2021). https://doi.org/10.1016/j.mcat.2021.111731
[10] Z. Shang, S. Li, L. Li, G. Liu, and X. Liang, "Highly active and stable alumina supported nickel nanoparticle catalysts for dry reforming of methane," Applied Catalysis B: Environmental, **201**, 302-309 (2017). https://doi.org/10.1016/j.apcatb.2016.08.019
[11] L. Liu, and A. Corma, "Metal catalysts for heterogeneous catalysis: from single atoms to nanoclusters and nanoparticles," Chemical reviews, **118**(10), 4981-5079 (2018). https://doi.org/10.1021/acs.chemrev.7b00776.
[12] T.K. Turdaliev, K.B. Ashurov, and R.K. Ashurov, "Morphology and Optical Characteristics of TiO2 Nanofilms Grown by Atomic-Layer Deposition on a Macroporous Silicon Substrate," Journal of Applied Spectroscopy, **91**(4), 769-774 (2024). https://doi.org/10.1007/s10812-024-01783-z
[13] I.J. Abdisaidov, S.G. Gulomjanova, I.K. Khudaykulov, and K.B. Ashurov, "The Low-Temperature Growth of Carbon Nanotubes Using Nickel Catalyst," East European Journal of Physics, (3), 355-358 (2024). https://doi.org/10.26565/2312-4334-2024-3-41
[14] F.A. Silva, V.M.M. Salim and T.S. Rodrigues, "Controlled Nickel Nanoparticles: A Review on How Parameters of Synthesis Can Modulate Their Features and Properties," Applied Chem. **4**(1), 86-106 (2024). https://doi.org/10.3390/appliedchem4010007
[15] P. Camilos, C. Varvenne, and C. Mottet, "Size and shape effects on chemical ordering in Ni–Pt nanoalloys," Physical Chemistry Chemical Physics, **26**(21), 15192-15204 (2024). https://doi.org/10.1039/D4CP00979G
[16] A.S. Al-Fatesh, N.A. Bamatraf, S.B. Alreshaidan, J.K. Abu-Dahrieh, N. Patel, A.A. Ibrahim, *et al*., "Cost-effective single-step synthesis of metal oxide-supported Ni catalyst for H_2-production through dry reforming of methane," Arabian Journal for Science and Engineering, **49**(6), 8031-8047 (2024). https://doi.org/10.1007/s13369-023-08576-0
[17] S. Mehravar, B.M. Garmejani, and S. Fatemi, "Nickel-Deposited Hexagonal Boron Nitride Composites via Chemical Vapor Deposition: Unlocking Enhanced Magnetic Properties for Advanced Technologies," Journal of Materials Chemistry C, **13**, 6823-6830 (2025). https://doi.org/10.1039/D4TC05281A
[18] X. Chen, Z. Li, Y. Zhao, C. Qi, S. Li, and F. Li, "Wetting and interfacial phenomena between a Ni-based superalloy and silica-based ceramic cores with $ZrSiO_4$ additions," Journal of Physics: Conference Series, **2671**(1), 012025 (2024). https://doi.org/10.1088/1742-6596/2671/1/012025
[19] B.C. Bayer, D.A. Bosworth, F.B. Michaelis, R. Blume, G. Habler, R. Abart, *et al*., "In situ observations of phase transitions in metastable nickel (carbide)/carbon nanocomposites," The Journal of Physical Chemistry C, **120**(39), 22571-22584 (2016). https://doi.org/10.1021/acs.jpcc.6b01555

АНАЛІЗ ТЕМПЕРАТУРНО-ЗАЛЕЖНИХ ПОВЕРХНЕВИХ ВЛАСТИВОСТЕЙ У СИСТЕМІ Ni/SiO2/Si ПІД ЧАС ЕЛЕКТРОННО-ПРОМЕНЕВОГО ОСАДЖЕННЯ

А.А. Рахімов, І.Х. Худайкулов, А.А. Ісматов, М.М. Аділов
Інститут іонно-плазмових та лазерних технологій імені У.А. Аріфова, Академія наук Узбекистану
100125, вул. Дурмон Юлі, 33, Ташкент, Узбекистан

У цьому дослідженні ми вивчали морфологічні властивості тонких плівок нікелю (Ni) у формі острівців, сформованих на підкладці SiOx/Si за допомогою методу електронно-променевого випаровування. Морфологію досліджували за допомогою скануючої електронної мікроскопії (СЕМ) та атомно-силової мікроскопії (АСМ). Зображення СЕМ аналізували за допомогою програмного забезпечення ImageJ для визначення розміру, щільності, розподілу та коефіцієнта покриття острівців. Результати показали сильну залежність морфології островів від температури підкладки: при 20°C острови мали неправильну форму з щільністю 103 мкм$^{-2}$, тоді як при 250°C та 500°C острови набували більш сферичної форми, а їх щільність збільшувалася до 751,8 та 1212,4 мкм$^{-2}$ відповідно. АСМ-аналіз підтвердив рівномірний розподіл островів та їх середню висоту (15,4 нм). EDS-аналіз виявив наявність та рівномірний розподіл елементів Si, O та Ni на поверхні. Ці результати підтверджують, що температура підкладки є критичним фактором у процесі формування островів.

Ключові слова: *наночастинки нікелю; оксид кремнію; електронно-променеве фізичне осадження з парової фази; морфологія шару; вакуум; поверхня підкладки; нанокаталізатор*